Research Paper

Iodide modulates protein damage induced by the inflammation-associated heme enzyme myeloperoxidase

Luke F. Gamon[a], Simon Dieterich[a], Marta T. Ignasiak[a,b], Verena Schrameyer[c], Michael J. Davies[a,*]

[a] *Dept. of Biomedical Sciences, University of Copenhagen, Copenhagen, Denmark*
[b] *Faculty of Chemistry, Adam Mickiewicz University, and Wielkopolska Center for Advanced Technologies Poznan, Poland*
[c] *Marine Biological Section, Department of Biology, University of Copenhagen, Denmark*

A B S T R A C T

Iodide ions (I^-) are an essential dietary mineral, and crucial for mental and physical development, fertility and thyroid function. I^- is also a high affinity substrate for the heme enzyme myeloperoxidase (MPO), which is involved in bacterial cell killing during the immune response, and also host tissue damage during inflammation. In the presence of H_2O_2 and Cl^-, MPO generates the powerful oxidant hypochlorous acid (HOCl), with excessive formation of this species linked to multiple inflammatory diseases. In this study, we have examined the hypothesis that elevated levels of I^- would decrease HOCl formation and thereby protein damage induced by a $MPO/Cl^-/H_2O_2$ system, by acting as a competitive substrate. The presence of increasing I^- concentrations (0.1–10 μM; i.e. within the range readily achievable by oral supplementation in humans), decreased damage to both model proteins and extracellular matrix components as assessed by gross structural changes (SDS-PAGE), antibody recognition of parent and modified protein epitopes (ELISA), and quantification of both parent amino acid loss (UPLC) and formation of the HOCl-biomarker 3-chlorotyrosine (LC-MS) (reduced by ca. 50% at 10 μM I^-). Elevated levels of I^- (> 1 μM) also protected against functional changes as assessed by a decreased loss of adhesion (eg. 40% vs. < 22% with > 1 μM I^-) of primary human coronary artery endothelial cells (HCAECs), to MPO-modified human plasma fibronectin. These data indicate that low micromolar concentrations of I^-, which can be readily achieved in humans and are readily tolerated, may afford protection against cell and tissue damage induced by MPO.

1. Introduction

Iodide (I^-) is an essential dietary mineral which plays a key role in thyroid function [1], where it is the major substrate for the heme enzyme thyroid peroxidase (also known as thyroperoxidase or iodide peroxidase), which generates the key hormones triiodothyronine (T_3) and thyroxine (T_4), from tyrosine (Tyr) residues present on thyroglobulin. I^- deficiency results in hypothyroidism, impaired mental and physical development, decreased fertility rate, and goiter [2]. While there are risks associated with excess consumption, I^- supplementation represents a simple, cheap and highly beneficial health intervention [3].

I^- is also a substrate for other mammalian heme peroxidases, including myeloperoxidase (MPO), a key enzyme released from

intracellular storage granules of activated neutrophils, monocytes and some tissue macrophages, as part of innate immune defence against invading pathogens [4,5]. MPO generates the highly reactive and damaging oxidant hypochlorous acid (HOCl) from hydrogen peroxide (H_2O_2) and chloride ions (Cl^-) in order to kill bacteria, yeast and other foreign materials, and low levels of MPO are known to be associated with chronic infections [4,5]. However, MPO can also oxidize other anions (e.g. Br^-, SCN^-, I^-, NO_2^-) as well as organic substrates [4,6,7].

Inappropriate production of HOCl and other oxidizing species by MPO (e.g. via sterile inflammation, excessive or inappropriate stimulation of the immune system) has been linked to a number of human inflammatory pathologies, including cardiovascular diseases, cystic fibrosis, asthma, kidney disease and a number of degenerative neurological conditions including Parkinson's and Alzheimer's diseases,

amongst others [4,5,8–11]. MPO is released extracellularly (i.e. into phagolysosomes or externally to the cell), and is known to bind avidly to negatively-charged macromolecules including proteins, proteoglycans and glycosaminoglycans of the extracellular matrix (ECM) [12,13]. HOCl reacts with high rate constants with biological targets, and particularly proteins [14,15], and would therefore not be expected to diffuse large distances from its site of generation [16]. This is likely to result in marked damage to ECM materials to which it is bound, or those in close proximity. Considerable data support this hypothesis, with extensive damage detected on ECM materials at sites of inflammation, including within the artery wall during the development of atherosclerosis [17]. Thus up to 70% of the oxidized proteins detected in human atherosclerotic lesions has been reported to be ECM derived [18], and considerable evidence also exists for modification of other extracellular materials including plasma proteins, and low- and high-density lipoproteins [19–22]. The ECM plays a critical role as the major load-bearing and structural component of tissues and is also a key determinant of cell binding, proliferation and migration, a reservoir for growth factors and cytokines, and a major modulator of enzyme activity and function [23,24]. Evidence has been presented for the presence of MPO mRNA, protein and enzymatic activity in cardiovascular lesions, together with evidence for protein damage and a strong association between the extent of HOCl-mediated damage and the severity of disease [8,25–27]. The detection of MPO in the shoulder regions of atherosclerotic lesions, which are susceptible to rupture (the major cause of many heart attacks and strokes) indicates that the damage induced by this enzyme may play a major role in such events [28,29]. Furthermore, strong associations have been reported between the levels of MPO and the diagnosis and severity of cardiovascular disease, with the levels of this enzyme being both diagnostic of the disease, and prognostic of adverse outcomes [30–32]. Consistent with these data, recent work has highlighted the potential of molecular imaging of MPO in determining high-risk atherosclerotic plaques [33,34].

Modulation of MPO activity have been proposed as a therapeutic approach in inflammatory diseases, as inhibition may reduce MPO-derived oxidative damage [35]. Thus both suicide and competitive inhibitors of MPO (e.g. benzoic acid hydrazides [36] and thioxanthines [37]), and alternative substrates (e.g. nitroxides [38], acetaminophen/paracetamol [39]) have been examined as potential modulators of MPO-derived damage (reviewed [10,40]). Whilst Cl^- is the most abundant MPO substrate, its oxidation by Compound I is relatively slow compared to Br^-, I^-, and SCN^- with apparent second order rate constants, at pH 7.0, of 2.5×10^4, 1.1×10^6, 7.2×10^6, and $9.6 \times 10^6\,M^{-1}\,s^{-1}$ for Cl^-, Br^-, I^- and SCN^- respectively [7]. Oxidation of SCN^- generates hypothiocyanous acid (HOSCN) [41]. HOSCN is a less powerful and less reactive oxidant than HOCl, with a high specificity for thiols (RSH, both free and in proteins), though these reactions occur at modest rates ($k \sim 10^4$ vs $\sim 10^8\,M^{-1}\,s^{-1}$ for reaction of Cys with HOSCN and HOCl, respectively) [42]. Increasing the concentration of SCN^- alters the ratio of HOCl to HOSCN formed by MPO, and can decrease biological damage [41,43,44]. SCN^- supplementation (via drinking water) of mice that express human MPO decreases the size of atherosclerotic lesions present in their arteries when fed a high-fat, high-cholesterol diet [45]. In addition, a retrospective analysis of people who suffered a first myocardial infarction with a subsequent 12 year follow-up, indicated that the lowest rates of subsequent all-cause mortality were in the group with low MPO levels and high SCN^-, and that high levels of SCN^- were associated with decreased mortality [46]. The extent of this effect cannot be ascertained completely, as this population contained both non-smokers, as well as ex- and current smokers, with the smokers have a known and significantly elevated risk of cardiovascular disease. However, despite this confounding factor, consideration of the data as a whole indicates that increasing SCN^- levels *in vivo* may afford protection against the development or progression of atherosclerosis.

Oxidation of I^- by Compound I of MPO is only marginally slower

than for SCN^-, and the resulting hypoiodous acid (HOI) has a much lower redox potential than HOCl (0.78 vs 1.28 V). Thus HOI would be expected to be both selective and less damaging than HOCl [47]. Several experimental and epidemiological studies have provided evidence for a protective effect of I^- in cardiovascular disease, but the underlying biochemical mechanism(s) are unclear [48]. Low urinary I^- concentrations have been associated with coronary artery disease in the North American National Health and Nutrition Examination Study (NHANES) [49], and recent work has shown that I^- can protect heart tissue against reperfusion injury-induced damage in a murine model [50]. This has been proposed to be due to metabolic changes [50], but MPO has also been strongly associated with reperfusion induced tissue injury as a result of neutrophil accumulation and activation after O_2 deprivation [51]. A role for I^- in modulating MPO-induced damage has poorly studied probably as a result of its low systemic concentration ($< 1\,\mu M$ for I^-, 100 mM for Cl^-, 20–80 μM for SCN^-) [52], though there is abundant evidence that I^- levels can be significantly elevated by interventions [53,54]. In the light of these data, we hypothesised that I^- might reduce oxidative damage induced by MPO, when I^- levels are elevated over typical physiologic levels. Here we provide evidence in support of this hypothesis, with increased I^- concentrations modulating protein damage induced by MPO. These findings illustrate the potential of I^- to minimize damage associated with MPO-mediated damage and chronic inflammation.

2. Materials and methods

2.1. Chemicals and reagents

Unless otherwise stated, all chemicals were purchased from commercial sources and used as received. UPLC buffers were prepared using HPLC grade methanol (VWR) and tetrahydrofuran (Chromasolv Plus, Sigma Aldrich). Aqueous solutions were prepared using MilliQ water and buffers were prepared from 0.5 M sodium phosphate buffer at pH 7.4, or PBS, and chelex-treated prior to use to remove trace metal ions. Cl^- and I^- solutions were prepared using NaCl and KI (Sigma Aldrich). The concentration of stock H_2O_2 and HOCl solutions (Sigma Aldrich) were determined spectrophotometrically (H_2O_2 in H_2O, ε_{240} 43.6 $M^{-1}\,cm^{-1}$; HOCl in 0.5 M NaOH, ε_{292} 350 $M^{-1}\,cm^{-1}$). Immunoblotting and ELISA were performed using the following monoclonal antibodies (mAb): anti-fibronectin A17 (ab26245, Abcam), anti-fibronectin A32 (CSI 005-32-02, Thermo Fisher Scientific), 2D10G9 (raised against HOCl-modified protein; a kind gift from A. Prof Ernst Malle, Medical University of Graz, Austria) and anti-dityrosine (Clone 1C3 monoclonal antibody, Nordic Biosite) [55]. Detection of immune complexes from immunoblotting was achieved with ECL anti-rabbit IgG horseradish peroxidase-linked whole antibody (NA934V, GE Healthcare UK). Detection for ELISA was achieved with a polyclonal rabbit anti-mouse IgG alkaline phosphate conjugated antibody (ab97043, Abcam).

2.2. Treatment of fibronectin with HOCl or MPO/H₂O₂/Cl⁻ system in the presence of I⁻

Human plasma fibronectin (0.228 μM final concentration for SDS-PAGE and immunoblotting, 1.14 μM for HPLC analysis) was diluted in phosphate buffer (0.1 M final concentration, pH 7.4) containing Cl^- (0.1 M) and I^- over the concentration range 0.01–400 μM. For the MPO/H_2O_2 system, a 500-fold molar excess of H_2O_2 over the enzyme concentration, was added in five equal aliquots to samples containing 100 nM MPO over a period of 10 min and incubated for 2 h at 37 °C.

2.3. Ultra high-performance liquid chromatography (UPLC)

Loss of parent amino acids was quantified by UPLC analysis with pre-column derivatization using *o*-phthaldialdehyde. Fibronectin

samples (25 μg of protein in 50 μL 0.1 M phosphate buffer) were hydrolysed using 4 M methanesulfonic acid as described previously [56], with minor modifications. Proteins were precipitated by the addition of 150 μL 10.67% (w/v) trichloroacetic acid and incubated at 4 °C for 15 min. After removal of the supernatant, the protein pellet was hydrolysed by the addition of 50 μL 4 M MSA containing 0.2% (w/v) tryptamine (Sigma Aldrich) and incubation for 16 h under vacuum at 110 °C. The samples were then neutralised with 55 μL freshly prepared 4 M NaOH, filtered using Nanosep MF 0.2 μm centrifugal filters and diluted 10-fold with 0.2 M aqueous sodium carbonate buffer, pH 10.3. Pre-column derivatization of the diluted samples (40 μL) was performed with OPA (40 μL, 1 mg mL^{-1} in 0.2 M aqueous sodium carbonate buffer pH 10.3, with 1 μL mL^{-1} 2-mercaptoethanol added prior to derivatization). Standard curves were generated using commercially-available amino acid mixtures. The fluorescently tagged amino acid derivatives were separated on a Shimadzu Nexera system using a Kinetex 2.6 μm EVO C18 100 Å LC column (150 × 3.0 mm) and eluted using a gradient system (Buffer A: 100 mM sodium acetate, pH 5.3 in water with 2.5% (v/v) tetrahydrofuran and 15% (v/v) methanol; Buffer B: 100 mM sodium acetate pH 5.3 in water with 2.5% (v/v) tetrahydrofuran and 80% (v/v) methanol). A flow rate of 0.8 mL min^{-1} was used, with the following gradient: 100% buffer A for 3 min, 0–10.5% buffer B linear gradient over 7.5 min, 10.5% buffer B for 5 min, 10.5–65% buffer B linear gradient over 3 min, 65–100% buffer B linear gradient over 1 min, 100% buffer B for 2 min, 100-0% buffer B linear gradient over 0.5 min, followed by equilibration at 100% buffer A for 3.5 min. The tagged amino acids were detected using a Shimadzu RF-20A fluorescence detector with λ_{ex} 340 nm and λ_{em} 440 nm.

2.4. SDS-PAGE and immunoblotting

Samples for SDS-PAGE analysis were prepared using NuPAGE LDS Sample Buffer (4x dilution) and NuPAGE Sample Reducing Agent (10x dilution) according to the manufacturer's instructions (Invitrogen). Protein samples were denatured by incubation at 70 °C for 10 min. Proteins were loaded at 0.5 μg per well for 12-well gels, and 0.375 μg per well for 15-well gels. HiMark™ pre-stained protein standards (31–460 kDa) were used as molecular mass markers. Electrophoresis was carried out on 1 mm NuPAGE NOVEX 3–8% Tris-Acetate Gels using NuPAGE Tris-Acetate SDS Running Buffer at 150 V for 70 min. Following electrophoretic separation, proteins were analysed using immunoblotting.

For immunoblotting, proteins were electroblotted onto PVDF membranes over a period of 7 min using an iBlot® transfer apparatus (Invitrogen). The membranes were blocked with 1% (w/v) BSA in TBS with Tween 20 (TBST) for 1 h and then incubated with primary antibody (A17, 1:10,000 and anti-dityrosine, 1:500) in blocking solution overnight at 4 °C. Membranes were then rinsed 3 times with TBST for 5 min before incubation with secondary HRP-conjugated antibody. Unbound antibody was removed by 4 washes with TBST for 10 min, and once with TBS for 10 min. Immune complexes were detected using Western Lightning Plus ECL reagent (NEL104001EA; Perkin Elmer, Waltham, MA, USA) and imaged using a G: BOX Chemi XR5 system (Syngene).

2.5. ELISA based analysis of loss of parent fibronectin epitopes and HOCl-mediated protein damage

Human plasma fibronectin (50 μL per well, 5 μg mL^{-1} in 0.1 M phosphate buffer, pH 7.4) was coated onto 96-well high-binding microtitre plates by incubation overnight at 4 °C. The wells were then washed twice with 200 μL PBS to remove any excess or non-bound fibronectin, then treated with MPO (20 nM), H$_2$O$_2$ (32 μM), Cl$^-$ (100 mM) and varying concentrations of I$^-$ in a total volume of 50 μL 0.1 M phosphate buffer, pH 7.4. After incubation at 37 °C for 2 h, the wells were washed twice with 200 μL PBS and blocked with 100 μL

0.1% casein (w/v) in PBS for 1 h at 21 °C. The wells were then washed twice with 200 μL PBS and incubated with 50 μL primary antibody (diluted in 0.1% casein (w/v) in PBS; A17 1:25,000, A32 1:2000, 2D10G9 1:100) overnight at 4 °C. Unbound antibody was removed by two washes with 200 μL PBST, and the wells were then incubated with 50 μL secondary antibody (Alkaline Phosphatase conjugated anti-mouse Ig in 0.1% casein (w/v) in PBS; 1:1000) for 1 h at 21 °C. Unbound secondary antibody was then removed by four washes with 200 μL TBST. TBST was employed for the final washes to avoid interference of phosphate in the Alkaline Phosphatase assay, in which 50 μL of Alkaline Phosphatase Yellow (*p*-nitrophenylphosphate, pNPP) substrate solution (Sigma Aldrich) was added to each well and the absorbance measured at 405 nm using a microplate reader (SpectraMax i3x Multi-Mode reader).

2.6. Determination of 3-chloro-ʟ-tyrosine by LC-MS

Protein samples (25 μg) were precipitated with TCA (8% w/v final concentration) and spiked with isotope-labelled 3-chloro-[^{13}C$_6$]tyrosine (100 pmol) before evaporation using a centrifugal vacuum concentrator for 1 h at 60 °C. The protein pellet was hydrolysed overnight in 4 M methanesulfonic acid (50 μL) under vacuum at 110 °C. The resulting liberated amino acids were partially purified by solid-phase extraction using 1 mL C-18 cartridges (Supelco), with the columns activated using 100% methanol (1 mL), followed by equilibration with 0.1% TFA in water (2 × 1 mL). Samples were diluted with 1% TFA in water (10 μL hydrolysate into 400 μL of 1% TFA) in order to improve ion-pairing and subsequent binding of amino acids to the C18 material. The samples were loaded onto the column and washed with 0.1% TFA in water (1 × 1 mL) followed by elution with 50% methanol containing 0.1% formic acid (1 × 1 mL). Extracts were dried at 60 °C under vacuum for 4 h and then redissolved in 50 μL 0.1% formic acid.

3-Chlorotyrosine (3-ClTyr) was quantified by ESI LC-MS in the positive ion mode using a Bruker Impact HD II mass spectrometer. Samples were separated by gradient elution using a Phenomenex Aeris™ 2.6 μm PEPTIDE XB-C18 250 × 2.1 mm HPLC column. The elution was initiated at 3% B for 1 min, followed by gradient elution from 3 to 50% B over 9 min, 50–80% B over 2 min, followed by isocratic elution using 80% B for 3 min, before decreasing to 3% B over 2 min and re-equilibration at 3% B for 3 min. Buffer A consisted of 0.1% formic acid in H$_2$O, and buffer B 80% acetonitrile in H$_2$O with 0.1% formic acid. The electrospray needle was held at 4500 V, with end plate offset of 500 V and temperature of 200 °C. Nitrogen gas was used for both the nebuliser (2.0 Bar) and as the dry gas (8.0 L min^{-1}). An external standard curve was generated for 3-ClTyr with 78 fmol–20 pmol loaded onto the column, with the internal standard maintained at a loading of 4 pmol. A linear response of 3-ClTyr relative to the internal standard was observed over this concentration range. Standards were prepared in 0.1% formic acid in H$_2$O. Spectra were collected in MS1 mode and quantification performed on extracted ion chromatograms for 3-ClTyr (*m/z* 216.04) and 3-chloro-[^{13}C$_6$]tyrosine (*m/z* 222.06).

2.7. Determination of H$_2$O$_2$ consumption by MPO

Consumption of H$_2$O$_2$ by MPO was determined in the presence of Cl$^-$ and varying amounts of I$^-$ using an H$_2$O$_2$-sensitive electrode (World Precision Instruments, HPO-ISO-2), as reported previously [38]. Solutions were prepared using 0.1 M sodium phosphate buffer, pH 7.4, with 50 μM H$_2$O$_2$ added, followed by 20 nM MPO. Methionine (250 μM) was included to quench the HOCl formed and prevent loss of enzyme activity. The removal of H$_2$O$_2$ was monitored until complete consumption. The rate of turnover was determined by using the initial linear sections of the H$_2$O$_2$ consumption curves, over a period of 120 s, after stabilization of the signal following MPO injection.

2.8. Cell adhesion centrifugation assay

Human plasma fibronectin (50 μL per well, 10 μg mL^{-1} in 0.1 M phosphate buffer at pH 7.4) was coated onto a 96-well tissue-culture treated, clear-bottom, black well plates by incubation overnight at 4 °C. The wells were washed twice with 200 μL PBS to remove excess or non-bound fibronectin, then treated with MPO (20 nM), H$_2$O$_2$ (64 μM), Cl$^-$ (100 mM) and varying concentrations of I$^-$ in a total volume of 50 μL 0.1 M phosphate buffer, pH 7.4. Following incubation at 37 °C for 2 h, the wells were washed twice with 200 μL DPBS and blocked for 30 min at 21 °C with 100 μL BSA in DPBS (1% w/v, heat-denatured at 85 °C for 12 min, sterile-filtered). The wells were then washed twice with 200 μL DPBS to remove blocking solution, and human coronary artery endothelial cells added (Cell Applications, San Diego, CA, USA; 20,000 cells well^{-1} in 50 μL basal media, pre-loaded with Calcein-AM at 5 μM in basal media for 30 min). The cells were allowed to adhere for 2 h in an incubator at 37 °C. The wells were then overfilled with HBSS (with Mg^{2+}/Ca^{2+}), sealed with adhesive foil and placed upside down in a centrifuge. The plate was centrifuged at 40 g for 5 min followed by removal of the supernatant containing unbound cells by inversion of the plate. Relative cell density was obtained by measurement of Calcein-AM fluorescence (λ_{ex} 485 nm, λ_{em} 525 nm) using a microplate-reader (SpectraMax i3x Multi-Mode reader, 12-point measurement, average of 4 technical replicates).

2.9. Determination of iodate as generated by the MPO/H$_2$O$_2$/Cl$^-$ system

Iodate was quantified by reaction with an excess of KI in H$_2$SO$_4$/H$_3$BO$_3$ via the Villermaux-Dushman reaction (iodate/iodide variation of the iodine-clock reaction) [57]. Briefly, MPO (20 nM) was reacted with H$_2$O$_2$ (64 μM) in the presence of Cl$^-$ (100 mM) and varying concentrations of I$^-$ in a total volume of 1 mL 0.1 M phosphate buffer, pH 7.4. Reactions were performed with, or without, BSA (50 nM) as a scavenger for generated HOCl/HOI. Following incubation at 37 °C for 2 h, the solutions were passed through a C18 cartridge to remove enzyme/protein (Supelco) and acidified by addition of 0.2 M H$_2$SO$_4$ (2:1, sample:H$_2$SO$_4$). IO$_3^-$ in the solution was then determined spectrophotometrically as I$_2$ at 288 nm by reaction with KI (60 mM) in a solution of aqueous H$_3$BO$_3$ (100 mM). A standard curve was prepared with KIO$_3$ at concentrations of 5–100 μM. Reactions were performed in triplicate.

2.10. Determination of chloramines as generated by the MPO/H$_2$O$_2$/Cl$^-$ system

The presence of chloramines generated by MPO was determined using a TNB assay [56]. Briefly, taurine (40 mM) was incubated at 37 °C for 30 min with varying concentrations of IO$_3^-$ (0–40 μM) and an MPO/H$_2$O$_2$/Cl$^-$ system. Reactions were performed in the presence of 0.1 M sodium phosphate buffer at pH 7.4, MPO (100 nM), Cl$^-$ (100 mM) and H$_2$O$_2$ (50 μM). The reaction was stopped by addition of catalase and chloramines determined by reaction with TNB (generated from hydrolysis of DTNB in 50 mM NaOH) and consumption of TNB measured using a microplate-reader ($\varepsilon_{412nm} = 14,150$ M^{-1} cm^{-1}).

2.11. Statistical analysis

Experiments were performed as independent triplicates, unless otherwise indicated, and errors are presented as standard deviation of the mean. Statistical analyses were performed using GraphPad Prism 7 for Mac (GraphPad Software, San Diego, CA, USA) with p < 0.05 taken as significant. One-way analysis of variance (ANOVA) with Dunnett's post hoc test was used to compare the effects of MPO/Cl$^-$/H$_2$O$_2$ treated samples to the control (no I$^-$) and the subsequent effect of increasing I$^-$ concentrations. Student's t-tests were used to compare untreated samples with the control treatment (no I$^-$).

3. Results

3.1. I$^-$ protects against damage to functional regions of human fibronectin induced by MPO/Cl$^-$/H$_2$O$_2$

Exposure of human fibronectin to increasing concentrations of HOCl has been shown previously to result in chlorination of tyrosine (Tyr) residues and oxidation at cysteine (Cys), methionine (Met) and tryptophan (Trp) residues [58,59]. The effect of I$^-$ on these modifications was therefore examined in reaction systems in which human plasma fibronectin (0.228 μM) was exposed to MPO (100 nM)/H$_2$O$_2$ (50 μM)/Cl$^-$ (100 mM) using a microplate-based ELISA method to examine alterations to functional epitopes on the protein.

In the absence of I$^-$, a significant loss of epitope recognition of both the cell binding region (mAb A17, 38.3 ± 5.6% loss versus control) and heparin binding region (mAb A32, 50.3 ± 9.0% loss versus control) was observed after exposure of the fibronectin to the MPO/Cl$^-$/H$_2$O$_2$ system. The presence of increasing concentrations of I$^-$ resulted in a decreased loss of epitope recognition to levels of ca. 90% for both antibodies, with this being statistically-significant for 1–100 μM I$^-$. The small decrease in antibody recognition at very high I$^-$ concentrations (50–100 μM) was not statistically significant.

The formation of modified epitopes on fibronectin was probed with mAb 2D10G9 which recognises HOCl-modified proteins [25,26,60–62]. Untreated fibronectin, BSA and HSA (used as controls) showed only very low background signals. After exposure to the MPO/Cl$^-$/H$_2$O$_2$ system, the oxidant-treated samples showed significant recognition by 2D10G9, consistent with significant HOCl-mediated damage (Fig. 1C). The presence of increasing concentrations of I$^-$ resulted in decreased recognition by 2D10G9, consistent with lower extents of damage, with this being significant at I$^-$ concentrations > 0.1 μM. Whilst 2D10G9 also recognise HOBr-induced damage [34], the current results suggest that this antibody does not recognise HOI-mediated protein damage, though the exact epitope recognised by this antibody is poorly defined [25,34].

3.2. Structural changes to human fibronectin induced by the MPO/Cl$^-$/H$_2$O$_2$ system in the presence of I$^-$

In order to investigate the effect of I$^-$ upon MPO-mediated changes in protein structure, fibronectin (1 μM) was treated with MPO (0.1 μM)/H$_2$O$_2$ (500 μM)/Cl$^-$ (100 mM) in the absence or presence of varying concentrations of I$^-$ (0–400 μM). Effects on fibronectin structure were probed by SDS-PAGE followed by immunoblotting. In the presence of MPO/H$_2$O$_2$/Cl$^-$, additional bands were detected by immunoblotting using mAb A17, at masses higher and lower that the parent protein fibronectin, which appears as a single broad band due to the similarity in masses of the two (α and β) chains under reducing conditions (c.f. lanes 1 vs. 12 in Fig. 2). The presence of low concentrations of I$^-$ (0.01–0.5 μM) did not give rise to significant changes (Fig. 2), whereas with higher I$^-$ levels (1–5 μM) a small decrease in the intensity of staining of both the higher and lower mass bands were detected, together with a more intense staining of the parent protein band. At very high concentrations of I$^-$ (> 100 μM) a marked increase in fibronectin fragmentation and aggregation was detected, together with a loss of recognition of the parent protein band. These changes are consistent with a reduction in protein damage at low I$^-$ concentrations, and a higher extent of modification with very high levels of I$^-$. The presence of protein bands at ca. 460 kDa is consistent with the formation of fibronectin homo- and hetero-dimers (α-α, β-β, α-β). As these samples were analysed under reducing conditions, these higher molecular mass species are unlikely to be disulfide-bonded species. Protein samples prepared and separated under identical conditions, and probed using an antibody against di-tyrosine, did not give positive staining, suggesting that these aggregates do not arise via the formation of this particular cross-link (data not shown). The identity of the cross-links
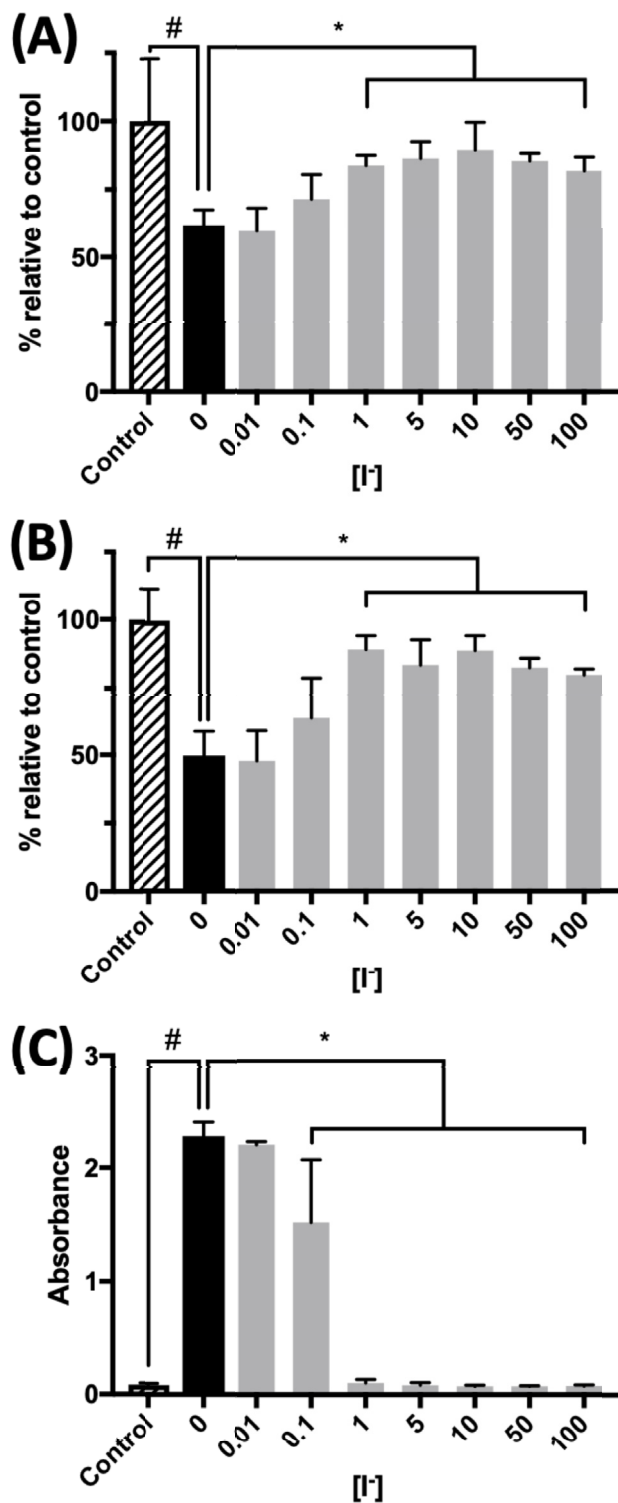
Fig. 1. ELISA based detection of HOCl-mediated damage to human plasma fibronectin incubated with a MPO/H_2O_2/Cl^- system, in the absence or presence of I^-. Antibodies were used to detect (A) damage to the cell-binding fragment (anti-fibronectin mAb A17), (B) damage to the heparin-binding region (anti-fibronectin mAb A32), and (C) HOCl-induced damage (mAb 2D10G9, raised against HOCl-modified protein). Human plasma fibronectin (2.5 μg in 50 μL) was treated with MPO (20 nM), H_2O_2 (32 μM), Cl^- (100 mM) for 2 h at 37 °C in 0.1 M phosphate buffer, pH 7.4. Data are presented as mean + SD from 3 independent experiments. # Indicates statistical significance of the control against the oxidized sample in the absence of I^- (0 μM I^-) as determined by Student's t-test. * Indicates statistical significance against the oxidized sample in the absence of I^- (0 μM I^-), as determined by one-way ANOVA with post-hoc analysis using Dunnett's multiple comparison test.
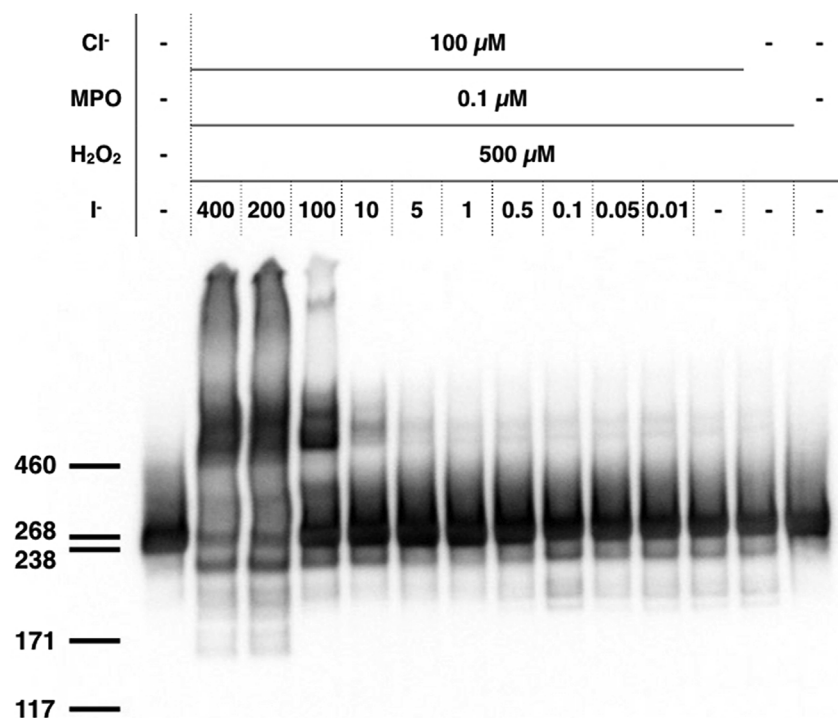
Fig. 2. Structural changes induced on human plasma fibronectin induced by incubation with a MPO/H_2O_2/Cl^- system in the presence of I^-, detected by Western-blot following SDS-PAGE separation under reducing conditions. The blot was probed for recognition of the cell-binding region of fibronectin using anti-Fibronectin mAb A17 and subsequent chemiluminescence detection (see Materials and Methods). The major bands detected are from the monomer bands of fibronectin. A representative blot is presented.

therefore remains unresolved, though these are likely to be carbon-carbon linked dimers.

3.3. Quantification of amino acid oxidation and 3-chlorotyrosine formation on fibronectin induced by MPO/Cl^-/H_2O_2 in the presence of varying concentrations of I^-

The effect of increasing I^- concentrations on MPO-mediated oxidation of amino acids present on fibronectin was investigated using UPLC analysis of hydrolysed fibronectin samples. Fibronectin (25 μg in 50 μL 0.1 M phosphate buffer) was incubated with MPO/Cl^-/H_2O_2 (as described above) in the absence and presence of varying concentrations of I^-, prior to total amino acid analysis. In the absence of I^-, the levels of Met and Trp were decreased, relative to the untreated protein, on exposure to MPO/Cl^-/H_2O_2. All other amino acid residues examined were not significantly affected. In the presence of increasing levels of I^- the loss of Met was decreased in a dose-dependent manner, with this being statistically significant at > 10 μM I^- (Fig. 3). No significant change was detected for Trp, though a trend towards a decreased loss was apparent (Fig. 3). While no significant loss of Tyr was detected with MPO/Cl^-/H_2O_2 in the absence of I^-, the presence of high concentrations of this ion (200–400 μM) resulted in a statistically-significant decrease of this amino acid.

We have recently shown that human plasma fibronectin is readily modified by MPO-derived HOCl and results in significant chlorination of the protein at Tyr residues, giving both 3-chloroTyr (3-ClTyr) and 3,5-dichloroTyr [58]. Consequently the absolute concentrations of 3-ClTyr formed on both fibronectin and BSA (as a positive control and for comparison with previous data) were determined in both the absence and presence of increasing I^- concentrations, using LC-MS. The levels of 3-ClTyr were markedly elevated on both proteins on treatment with MPO/Cl^-/H_2O_2 in the absence of I^-, with the levels detected on BSA (ca. 450 nM, 6.5 nmol mg^{-1} protein) consistent with previous data [44,63]. Higher levels were detected on fibronectin (ca. 3 μM, 31 nmol mg^{-1} protein). The presence of I^- in both the fibronectin and BSA systems decreased 3-ClTyr levels in a dose-dependent manner, with the decrease statistically-significant at ≥ 10 μM I^- (Fig. 4). These data

are consistent with the mAb 2D10G9 antibody studies (Fig. 1C).

3.4. I^- improves adhesion of human coronary artery endothelial cells (HCAECs) to oxidized fibronectin in the MPO/Cl^-/H_2O_2 system

Previous data indicate that human coronary artery endothelial cells (HCAEC) adhere less well to HOCl-modified fibronectin when compared to native fibronectin, and also have altered gene expression in response to the modified protein [59]. Consequently, cell adhesion assays were performed to test whether the presence of I^- in the MPO/H_2O_2/Cl^- system could decrease the loss of cell adhesion arising from HOCl-induced modification. Treatment of fibronectin with the MPO/Cl^-/H_2O_2 system in the absence of I^- resulted in decreased HCAEC adhesion (60 ± 1.9% relative to non-oxidized control). The presence of low concentrations of I^- decreased this loss of function in a dose-dependent manner, with this being statistically significant at ≥ 1 μM (Fig. 5).

3.5. Myeloperoxidase activity is perturbed by high concentrations of I^-

The data presented above indicate that I^- at low concentrations can reduce the extent of damage induced by MPO/H_2O_2/Cl^- reaction systems. One potential rationale for these effects is potential (reversible or irreversible) inhibition of the MPO catalytic cycle, or by other secondary reactions involving I^-. In order to test these possibilities, the catalytic turnover of MPO was quantified, as measured by H_2O_2 consumption (using a H_2O_2-sensitive electrode) in the presence of Cl^- (100 mM), Met (250 μM, as a scavenger for HOCl to prevent enzyme auto-inactivation), and the absence and presence of increasing concentrations of I^-. H_2O_2 (50 μM) was introduced into a phosphate-buffered solution containing Cl^- (100 mM) and I^- (0, 1, 10, 25, 100 μM), and the reaction initiated by the addition of MPO (20 nM). Under these conditions the formation of Compound I, by reaction of the native enzyme with the added H_2O_2 is rapid, and the turnover of the enzyme is limited by the reaction of Compound I with Cl^- or I^-. No direct reaction between H_2O_2 and I^- was observed prior to the addition of MPO. In the absence of I^-, H_2O_2 was consumed at a rate of 3.5 μM min^{-1}

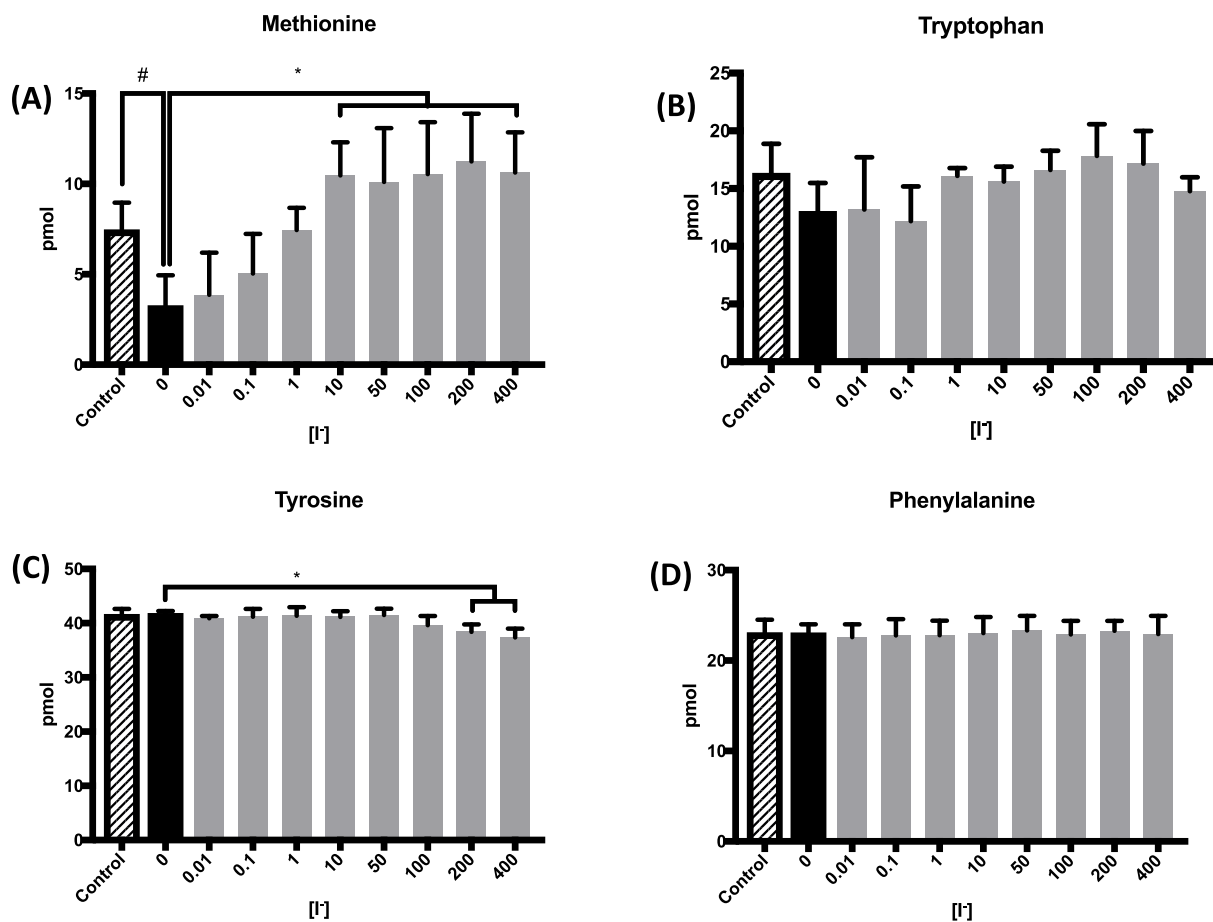**Methionine**

Tryptophan

Tyrosine

Phenylalanine

Fig. 3. UPLC quantification of (A) Met, (B) Trp, (C) Tyr and (D) Phe on human plasma fibronectin (5.68 μM) following treatment with MPO/H_2O_2/Cl^- in the absence or presence of I^-. Human plasma fibronectin (25 μg in 50 μL, 1.14 μM) was treated with MPO (100 nM), H_2O_2 (500x excess, 570 μM), Cl^- (100 mM) in the absence or presence of increasing I^- (0–400 μM) for 2 h at 37 °C in 0.1 M phosphate buffer, pH 7.4. Data are presented as mean + SD of three independent experiments. # Indicates statistical significance of the control against the oxidized sample in the absence of I^- (0 μM I^-) as determined by Student's t-test. * Indicates statistical significance against the oxidized sample in the absence of I^- (0 μM I^-) as determined by one-way ANOVA with post-hoc analysis using Dunnett's multiple comparison test.
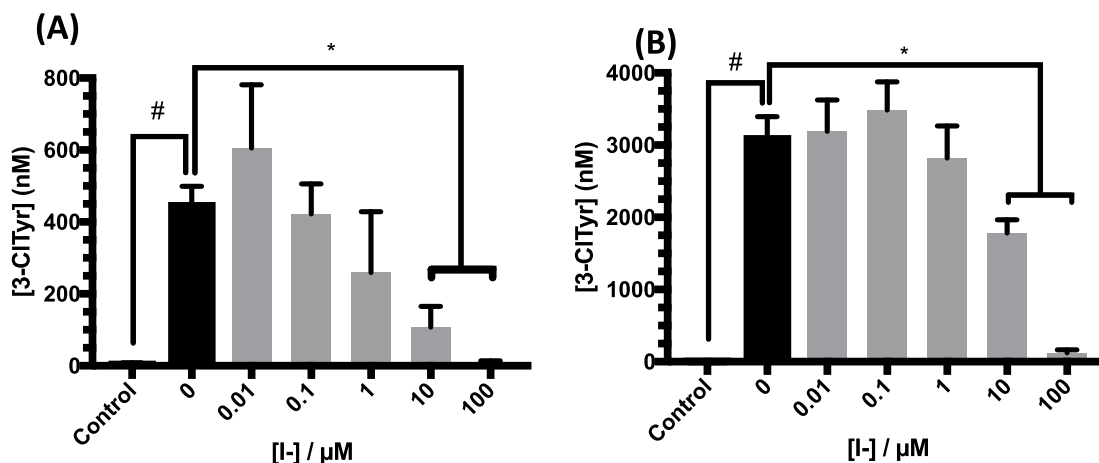
Fig. 4. Quantification of 3-ClTyr on (A) BSA, and (B) human plasma fibronectin, following treatment with MPO/H_2O_2/Cl^- in the presence of I^-. BSA or human plasma fibronectin (25 μg in 50 μL, 1.14 μM) were incubated with MPO (100 nM), H_2O_2 (500x excess, 570 μM), Cl^- (100 mM) in the absence or presence of increasing concentrations of I^- (0–400 μM) for 2 h at 37 °C in 0.1 M phosphate buffer, pH 7.4, before analysis by LC-MS. Data are presented as mean + SD from three independent experiments. # Indicates statistical significance of the control against the oxidized sample in the absence of I^- (0 μM I^-) as determined by Student's t-test. * Indicates statistical significance against the oxidized sample in the absence of I^- (0 μM I^-) as determined by one-way ANOVA with post-hoc analysis using Dunnett's multiple comparison test.
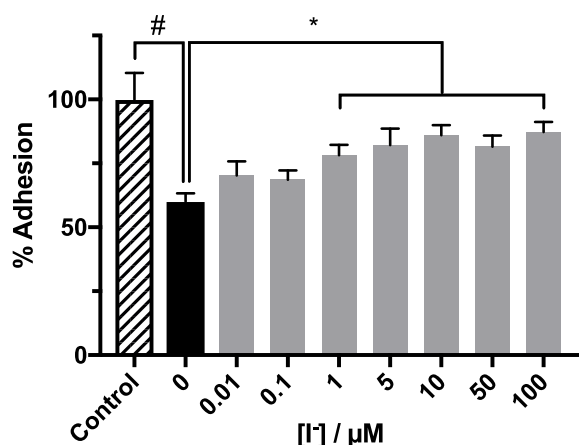
Fig. 5. Adhesion of human coronary artery endothelial cells (HCAECs) to fibronectin pretreated with a MPO/H_2O_2/Cl^- system in the absence or presence of I^-. Human plasma fibronectin (2.5 μg in 50 μL) was coated onto a 96-well plate and treated with MPO (20 nM), H_2O_2 (32 μM), Cl^- (100 mM) for 2 h at 37 °C in 0.1 M phosphate buffer, pH 7.4. Wells were washed with DPBS and blocked with 1% denatured-BSA in DPBS. HCAECs pre-stained with Calcein-AM (5 μM) were added and allowed to adhere for 2 h. Non-adherent cells were then removed by centrifugation at 40*g* for 5 min. Adherent cells were subsequently quantified by fluorescence of the Calcein-AM dye as described in the Materials and methods. Data are presented as mean + SD from three independent experiments. # Indicates statistical significance of the control against the oxidized sample in the absence of I^- (0 μM I^-) as determined by Student's t-test. * Indicates statistical significance against the oxidized sample in the absence of I^- (0 μM I^-) as determined by one-way ANOVA with post-hoc analysis using Dunnett's multiple comparison test.

(Fig. 6) The presence of low concentrations of I^- did not significantly perturb this rate, with only concentrations of $I^- \geq 25$ μM, found to significantly enhance the turnover of MPO, with consumption rates of 5.7 and 7.5 μM min^{-1} detected at 25 and 100 μM respectively (Fig. 6).

3.6. Determination of iodate (IO_3^-) formation by the MPO/Cl^-/H_2O_2 system

As MPO does not appear to be significantly inhibited by low concentrations of I^-, the potential formation of iodate (IO_3^-), a known oxidation product of I^-, was examined and quantified, as well as the potential perturbation of MPO activity by this species. Previous studies

Table 1
Quantification of iodate (μM) generated from reagent HOCl or HOCl generated by the MPO system in the absence and presence of I^- and BSA. HOCl was generated through reaction of MPO (100 nM), H_2O_2 (100 μM), I^- (100 μM) and Cl^- (100 mM) for 2 h at 37 °C in 0.1 M phosphate buffer, pH 7.4, with or without BSA (50 nM). Presence of I^- in the reaction mixture was confirmed by addition of HOCl (100 μM) and quantification of IO_3^- (via disproportionation of HOI). The determination of IO_3^- was performed by spectrophotometric assay with an excess of KI under acidic conditions. Data are presented as mean ± SD of three experimental replicates. LOD: limit of detection. *Theoretical yield: 33 μM.

Oxidation system	Concentration of IO_3^- detected/μM		
	I^- alone	MPO + H_2O_2 + I^- + Cl^-	
	−BSA	−BSA	+BSA
−HOCl	< 2 (LOD)	< 2 (LOD)	< 2 (LOD)
+HOCl	33.0 ± 0.6 *	33.7 ± 0.2	33.7 ± 0.5

have postulated that reaction of I^- with either the MPO/H_2O_2/Cl^- system, or its product HOCl, forms HOI and hence IO_3^- via a rapid disproportionation reaction that regenerates a proportion of the I^- originally consumed (Equation (2)) [64]. These secondary products, such as IO_3^-, would be expected to be less reactive than HOI itself [65]. The formation of IO_3^- on reaction of HOCl with I^- was confirmed by spectrophotometric assay after reaction of HOCl (100 μM) with equimolar concentrations of I^- at 21 °C over a period of 20 min (Table 1). Under these conditions HOCl should be converted rapidly to HOI which will undergo moderately slow (quantitative) disproportionation to I^- and IO_3^- (Equations (1) and (2)) [64,66]. The concentration of IO_3^- detected was ca. 33 μM, consistent with the expected value of 33 μM predicted from this chemistry.

$$HOCl + I^- \rightarrow HOI + Cl^- \tag{1}$$

$$3HOI \rightarrow IO_3^- + 2I^- + 3H^+ \tag{2}$$

IO_3^- generation was also examined after incubation of MPO with H_2O_2 (100 μM), Cl^- (100 mM) and I^- (100 μM) at 37 °C over a period of 2 h. The concentration of IO_3^- detected was below the limit of detection of the assay (2 μM) in both the absence and presence of 50 nM BSA (as a potential target for IO_3^-). Subsequent bolus addition of HOCl (100 μM) to these reactions, to oxidize any residual I^-, resulted in the detection of ca. 34 μM IO_3^- in both the absence and presence of BSA (Table 1). These data suggest that most of the initial I^- is not converted
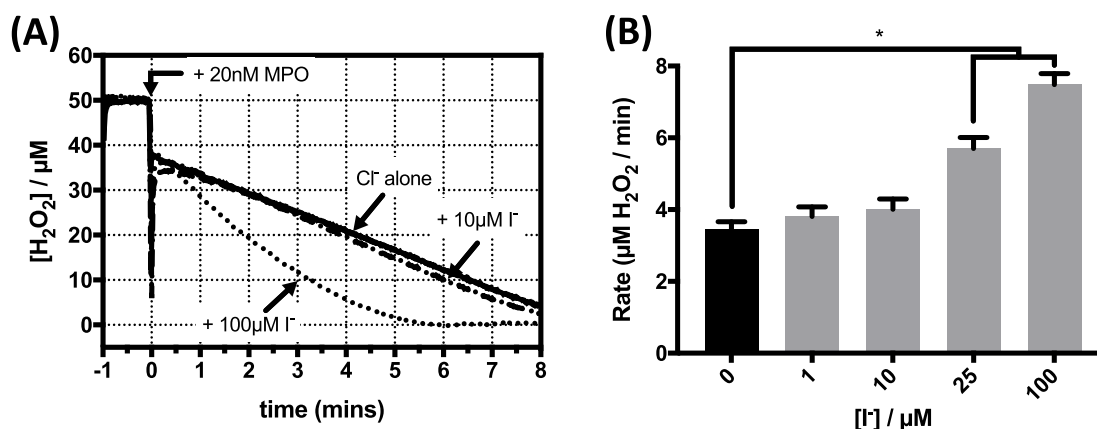

Fig. 6. Consumption of H_2O_2 over time detected using a H_2O_2-sensitive electrode (HPO-ISO-2) in the absence and presence of the MPO system in the absence or presence of the indicated concentrations of I^-. MPO (20 nM) was spiked into a solution of Cl^- (100 mM) and H_2O_2 (50 μM) in 0.1 M sodium phosphate buffer at pH 7.4. Reactions were performed at 25 °C. Panel (A) shows representative time course data (from 3 independent experiments) for H_2O_2 consumption. Panel (B) shows the rate of H_2O_2 consumption as determined by the slope of the curve over the first 120 s following stabilization of the signal after injection of MPO. Data in panel (B) are presented as mean + SD from 3 independent experiments, with * indicating statistical significance against the oxidized sample in the absence of I^- (0 μM I^-) as determined by one-way ANOVA with post-hoc analysis using Dunnett's multiple comparison test.
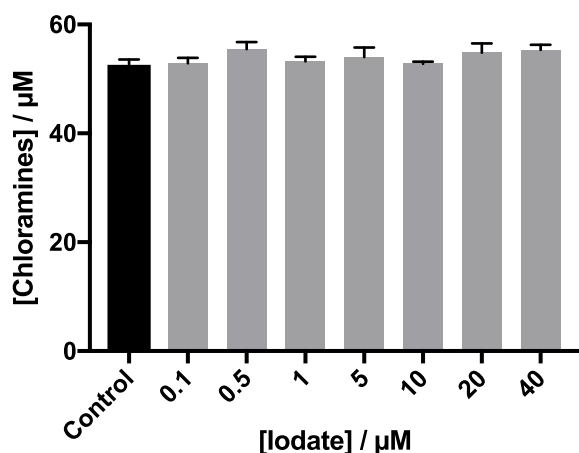
Fig. 7. Concentration of chloramine detected on taurine as determined using the TNB assay (see Materials and methods) after reaction of taurine (40 mM) with MPO (100 nM), H_2O_2 (50 μM), and Cl^- (100 mM) in 0.1 M sodium phosphate buffer, pH 7.4, in the absence and presence of varying concentrations of IO_3^-. Data are presented as mean + SD from 3 independent experiments. No statistical significance was detected between the samples as assessed by one-way ANOVA with post-hoc analysis using Dunnett's multiple comparison test.

to IO_3^-, or other products, during incubation with MPO/H_2O_2/Cl^-.

As IO_3^-, even if formed at low levels, might act as an MPO inhibitor, the activity of MPO was examined by determining the yield of chloramines formed from added taurine, by HOCl, using the TNB assay [56]. The yield of taurine chloramines was not perturbed by the presence of IO_3^-, at concentrations up to 40 μM, indicating that IO_3^- is not a significant inhibitor of MPO activity (Fig. 7).

4. Discussion

Multiple studies have demonstrated an association between MPO levels and outcomes of cardiovascular disease, with high levels indicative of poor health outcomes [67]. Previous work has shown that SCN^- can reduce the extent of MPO-induced damage on BSA and human plasma proteins, as judged by Met oxidation and 3-ClTyr formation, even in the presence of high Cl^- concentrations [44]. Other studies have also shown that damage to fibronectin can be attenuated by SCN^- [13], and that this anion can prevent damage in animal models of disease including cystic fibrosis and atherosclerosis [45,68,69]. Here we have examined whether I^-, another high affinity substrate for MPO, behaves in a similar manner, as I^- levels can be readily elevated in animals and humans by simple interventions. Such an activity might therefore have significant health benefits, and be readily applied.

Exposure of plasma fibronectin to HOCl and MPO/H_2O_2/Cl^- induces protein damage in a dose-dependent manner [58,59]. The residues modified by such exposure have been characterized by UPLC and MS peptide mass mapping, and include Tyr, Trp, His, Met and Cys/cystine [58]. Some of these modifications occur within functional (cell- and heparin-binding) domains, consistent with the loss of native epitopes, and altered functional properties including its capacity to act as a substrate for cell adherence and proliferation [58,59].

In the current study it has been demonstrated that such damage can be ameliorated by I^- at concentrations as low as 1 μM, with these low concentrations providing protection against modification to both the cell-binding and heparin-binding domains (Fig. 1A and B). Furthermore, the loss of cell adhesion to fibronectin induced by MPO/H_2O_2/Cl^- was also attenuated by low concentrations of I^- (Fig. 3).

Previous studies have shown that HOCl can modify the structure of fibronectin [59], with dose-dependent aggregation and fragmentation detected by SDS-PAGE with silver staining, and use of mAb A17 against

the cell-binding epitope. In contrast, the data presented here indicate that the species formed by the MPO/H_2O_2/Cl^- system in the presence of I^-, did not give rise to marked cross-linking or fragmentation of the protein, except at extremely high concentrations of I^-. Under the latter conditions significant smearing of the protein bands was detected to both lower and higher molecular masses, with the latter being particularly marked. These data indicate that HOI, the likely initial product of I^- oxidation, does not induce dramatic effects on the protein structure when formed at modest concentrations. In contrast, molecular iodine (I_2) or I_3^-, which may be formed from I^- by HOI at high concentrations, may be the source of these changes, with this occurring via iodination of Tyr (and possibly other residues) and cross-linking (possibly di-Tyr formation) (cf. the reactions of thyroid peroxidase) [70,71]. There is no evidence for the presence of such high I^- concentrations (> 100 μM; Fig. 2) at sites in inflammation, though they may occur in extreme cases of I^- overdoses. Even in the thyroid gland, where I^- is concentrated (to levels 20–50 times higher than those of plasma [72,73]) and used by thyroid peroxidase to iodinate thyroglobulin [70], these levels are below these that induce marked fibronectin damage.

Amino acids represent a major target for HOCl [74]. Under our conditions, most of the amino acids present in fibronectin were unaffected by the MPO/H_2O_2/Cl^- system, both in the absence and presence of I^-. The data obtained in the absence of I^- are in accord with previous reports for HOCl and MPO/H_2O_2/Cl^-, with stable (long-lived) modifications limited to Met, Cys/cystine, Trp, Tyr and His [58,59]. Reaction at amines, such as the ε-amino group of Lys side-chains, occurs at modest rates, but this yields unstable chloramines (RNHCl) [75], which would not be detected under the conditions used in these analyses. In the current study, oxidation of Met by the MPO/H_2O_2/Cl^- system was decreased in a dose-dependent manner by I^-. In contrast to previous and current MS studies (see above and below), no significant loss of Tyr was detected by UPLC, probably due to the insensitivity of this method at low levels of modification. However a small but significant loss of Tyr was detected by UPLC with the MPO/H_2O_2/Cl^- system with high I^- concentrations in agreement with previous data on the iodination of Tyr residues by peroxidases (Fig. 4A) [70].

The MS analyses showed significant formation of 3-ClTyr induced by MPO/H_2O_2/Cl^- on both fibronectin and the model protein BSA, with the levels of this biomarker decreased in a dose-dependent manner by increasing I^- concentrations. HOCl-mediated damage recognised by the mAb 2D10G9 (raised against HOCl-damaged low-density lipoproteins) was also significantly reduced in the presence of I^-, as determined by ELISA assay. As previous studies have shown that 3-ClTyr levels correlate with the severity of chronic kidney damage and cardiovascular disease [76], modulation of the formation of this biomarker may be of clinical significance.

Fibronectin and MPO have been shown previously to colocalise in diseased tissue [59], and MPO has also been shown to colocalise with HOCl-modified proteins in atherosclerotic plaques [34,77]. Furthermore, proteins immunoprecipitated with mAb 2D10G9 (i.e. species damaged by HOCl) have been shown to be recognised by fibronectin antibodies and to migrate on gels at the expected masses for fibronectin chains, consistent with fibronectin modification by MPO/H_2O_2/Cl^- in human atherosclerotic lesions [59]. Increased I^- levels *in vivo* may therefore reduce the amount of tissue damage induced by MPO. These results provide a novel mechanism which rationalizes the improved outcomes observed in animals (mice, rats and pigs) administered I^- prior to induction of an acute myocardial infarction [50,78].

While I^- is a high affinity substrate for MPO, the mechanism through which I^- reduces damage to fibronectin (and also BSA) is yet to be fully elucidated. Although the rate constants for reaction of Cl^- with Compound I of MPO is much lower than that for I^-, the high plasma concentrations of Cl^- would be expected to more than compensate for this, and hence with normal physiologic anion concentrations, Cl^- would be expected to outcompete I^- as a substrate [7]. In the case of SCN^-, the rate constants for reaction of this anion and I^- with

Compound I are similar, and therefore the higher concentrations of SCN^- compared to I^- in plasma, would also be expected to limit I^- oxidation. These data therefore suggest that competitive reaction of I^- with Compound I may not be the sole factor responsible for the decreased damage observed with increasing I^- concentrations, assuming the published rate constants for reactions of Compound I are correct.

A second potential explanation for the observed reduction in damage is via direct oxidation of I^- with HOCl, with consequent consumption of the latter (Equation (1)). This reaction is rapid [66] and hence should compete with protein targets for HOCl (cf. k for reaction with Cys of $3 \times 10^8 \, M^{-1} \, s^{-1}$) [79]. However, the data reported here indicate that statistically-significant protection occurs with I^- concentrations that considerably below the concentrations of HOCl that are likely to be formed from the H_2O_2 provided to MPO. Under such conditions, I^- would only be expected to remove a limited amount of the HOCl formed, assuming that the stoichiometry of Equations (1) and (2) is correct. Thus, each mole of I^- would be expected to quench 3 mol of HOCl. Whilst conversion of HOI to IO_3^-, which is a far weaker oxidant than either H_2O_2, HOCl or HOI, might partially account for the sub-stoichiometric effects, the iodate assay data (Table 1) indicates that little IO_3^- is formed on reaction of $MPO/H_2O_2/Cl^-$ with I^-, and the spiking experiments with added HOCl (to convert remaining I^- to HOI and therefore IO_3^-) reveal that I^- is still present at high concentrations and is not converted to HOI or IO_3^-. Reactions with BSA provided similar data, indicating there is no significant consumption of I^- by the protein. IO_3^- also had no effect on chloramine formation (a marker of enzyme activity), consistent with recent observations that, in contrast to I^-, IO_3^- does not provide a benefit in a mouse model of reperfusion injury [50]. Our results (Fig. 7) imply that IO_3^-, even if formed transiently, does not have a significant inhibitory effect on MPO. These data indicate that direct scavenging of HOCl by I^- is unlikely to be the major damaging-limiting pathways, unless other, unknown, recycling reactions occur.

Potential inhibition of MPO activity by I^- also does not appear to be a major process as the concentrations of I^- that provide protection to fibronectin did not significantly perturb H_2O_2 consumption by MPO. These data therefore suggest that I^- does not directly inhibit MPO (e.g. by binding to and/or blocking the active site). These studies also indicate that direct oxidation of I^- by H_2O_2 is not a significant event, as no loss of H_2O_2 was observed upon addition of I^- in the absence of MPO; this is consistent with a slow reaction between these materials at the concentrations used here (Fig. 6A) and also previous data [80].

Interference with the catalytic cycle of MPO, and particularly removal of Compound I via conversion to Compound II via a one-electron (peroxidase cycle) reaction also appears unlikely, as although I^- has a modest one-electron reduction potential ($I^•/I^-$, +1.35 V), this value is greater than that the one-electron reduction potential of Compound I (+1.16 V) and hence thermodynamically unfavourable [6,81].

These arguments suggest that, rather than inhibiting the enzyme or acting as a competitive substrate, I^- act in a catalytic manner, via an unidentified very fast secondary reaction mechanism. Alternatively, it may be a more efficient substrate for the enzyme than previously indicated [7]. The precise mechanism giving rise to the observed protection by low micromolar concentrations of I^- therefore warrants additional study.

Irrespective of the precise mechanism, the data presented here indicate that I^- can reduce MPO-induced damage *in vitro* at concentrations that can be achieved physiologically, with amelioration of protein damage and loss of cell adhesion detected at I^- concentrations as low as 1 μM. This concentration can be readily achieved in humans by oral supplementation [53], and it is also possible that local *in vivo* concentrations of I^- may be higher than systemic values, and may therefore result in greater effects than previously suspected. These results indicate the need for further investigation of I^- as a therapeutic agent and, more specifically, whether the observed benefits of I^- supplementation in cardiovascular disease are a result of interactions with MPO and its oxidants.

Conflicts of interest

The authors declare no conflicts of interest with regard to the data presented.

Acknowledgements

References

[1] M.B. Zimmermann, The role of iodine in human growth and development, Semin. Cell Dev. Biol. 22 (6) (2011) 645–652.

[2] F. Delange, The Disorders Induced by Iodine Deficiency, 4 (1) (1994) 107–128.

[3] M.B. Zimmermann, P.L. Jooste, C.S. Pandav, Iodine-deficiency disorders, The Lancet 372 (9645) (2008) 1251–1262.

[4] M.J. Davies, C.L. Hawkins, D.I. Pattison, M.D. Rees, Mammalian heme peroxidases: from molecular mechanisms to health implications, Antioxidants Redox Signal. 10 (7) (2008) 1199–1234.

[5] S.J. Klebanoff, Myeloperoxidase: friend and foe, J. Leukoc. Biol. 77 (5) (2005) 598–625.

[6] J. Arnhold, P.G. Furtmuller, G. Regelsberger, C. Obinger, Redox properties of the couple compound I/native enzyme of myeloperoxidase and eosinophil peroxidase, Eur. J. Biochem. 268 (19) (2001) 5142–5148.

[7] P.G. Furtmuller, U. Burner, C. Obinger, Reaction of myeloperoxidase compound I with chloride, bromide, iodide, and thiocyanate, Biochemistry 37 (51) (1998) 17923–17930.

[8] S.J. Nicholls, S.L. Hazen, Myeloperoxidase and cardiovascular disease, Arterioscler. Thromb. Vasc. Biol. 25 (6) (2005) 1102–1111.

[9] T.M. Jeitner, M. Kalogiannis, B.F. Krasnikov, I. Gomolin, M.R. Peltier, G.R. Moran, Linking inflammation and Parkinson disease: hypochlorous acid generates parkinsonian poisons, Toxicol. Sci. 151 (2) (2016) 388–402.

[10] M.J. Davies, Myeloperoxidase-derived oxidation: mechanisms of biological damage and its prevention, J. Clin. Biochem. Nutr. 48 (1) (2010) 8–19.

[11] B.S. van der Veen, M.P.J. de Winther, P. Heeringa, Myeloperoxidase: molecular mechanisms of action and their relevance to human health and disease, Antioxidants Redox Signal. 11 (11) (2009) 2899–2937.

[12] S. Baldus, V. Rudolph, M. Roiss, W.D. Ito, T.K. Rudolph, J.P. Eiserich, K. Sydow, D. Lau, K. Szocs, A. Klinke, L. Kubala, L. Berglund, S. Schrepfer, T. Deuse, M. Haddad, T. Risius, H. Klemm, H.C. Reichenspurner, T. Meinertz, T. Heitzer, Heparins increase endothelial nitric oxide bioavailability by liberating vessel-immobilized myeloperoxidase, Circulation 113 (15) (2006) 1871–1878.

[13] M.D. Rees, L. Dang, T. Thai, D.M. Owen, E. Malle, S.R. Thomas, Targeted subendothelial matrix oxidation by myeloperoxidase triggers myosin II-dependent de-adhesion and alters signaling in endothelial cells, Free Radic. Biol. Med. 53 (12) (2012) 2344–2356.

[14] D.I. Pattison, M.J. Davies, Absolute rate constants for the reaction of hypochlorous acid with protein side chains and peptide bonds, Chem. Res. Toxicol. 14 (10) (2001) 1453–1464.

[15] D.I. Pattison, M.J. Davies, C.L. Hawkins, Reactions and reactivity of myeloperoxidase-derived oxidants: differential biological effects of hypochlorous and hypothiocyanous acids, Free Radic. Res. 46 (8) (2012) 975–995.

[16] C.C. Winterbourn, Reconciling the chemistry and biology of reactive oxygen species, Nat. Chem. Biol. 4 (5) (2008) 278–286.

[17] A. Nikolaos, D. Spyridon, B. Georgios, G. Georgios, T. Dimitrios, A. Christos, K. Andreas, S. Christodoulos, Myeloperoxidase: expressing inflammation and oxidative stress in cardiovascular disease, Curr. Top. Med. Chem. 13 (2) (2013) 115–138.

[18] A.A. Woods, S.M. Linton, M.J. Davies, Detection of HOCl-mediated protein oxidation products in the extracellular matrix of human atherosclerotic plaques, Biochem. J. 370 (Pt 2) (2003) 729–735.

[19] S.L. Hazen, J.W. Heinecke, 3-Chlorotyrosine, a specific marker of myeloperoxidase-catalyzed oxidation, is markedly elevated in low density lipoprotein isolated from human atherosclerotic intima, J. Clin. Investig. 99 (9) (1997) 2075–2081.

[20] S.J. Nicholls, L. Zheng, S.L. Hazen, Formation of dysfunctional high-density lipoprotein by myeloperoxidase, Trends Cardiovasc. Med. 15 (6) (2005) 212–219.

[21] L. Zheng, B. Nukuna, M.-L. Brennan, M. Sun, M. Goormastic, M. Settle, D. Schmitt, X. Fu, L. Thomson, P.L. Fox, H. Ischiropoulos, J.D. Smith, M. Kinter, S.L. Hazen, Apolipoprotein A-I is a selective target for myeloperoxidase-catalyzed oxidation and functional impairment in subjects with cardiovascular disease, J. Clin. Investig. 114 (4) (2004) 529–541.

[22] C. Bergt, S. Pennathur, X. Fu, J. Byun, K. O'Brien, T.O. McDonald, P. Singh,

G.M. Anantharamaiah, A. Chait, J. Brunzell, R.L. Geary, J.F. Oram, J.W. Heinecke, The myeloperoxidase product hypochlorous acid oxidizes HDL in the human artery wall and impairs ABCA1-dependent cholesterol transport, Proc. Natl. Acad. Sci. U. S. A. 101 (35) (2004) 13032–13037.

[23] M.J. Chow, R. Turcotte, C.P. Lin, Y. Zhang, Arterial extracellular matrix: a mechanobiological study of the contributions and interactions of elastin and collagen, Biophys. J. 106 (12) (2014) 2684–2692.

[24] H. Ju, I.M. Dixon, Extracellular matrix and cardiovascular diseases, Can. J. Cardiol. 12 (12) (1996) 1259–1267.

[25] H.J. Grone, E.F. Grone, E. Malle, Immunohistochemical detection of hypochlorite-modified proteins in glomeruli of human membranous glomerulonephritis, Lab. Investig. 82 (1) (2002) 5–14.

[26] L.J. Hazell, L. Arnold, D. Flowers, G. Waeg, E. Malle, R. Stocker, Presence of hypochlorite-modified proteins in human atherosclerotic lesions, J. Clin. Investig. 97 (6) (1996) 1535–1544.

[27] L.J. Hazell, G. Baernthaler, R. Stocker, Correlation between intima-to-media ratio, apolipoprotein B-100, myeloperoxidase, and hypochlorite-oxidized proteins in human atherosclerosis, Free Radic. Biol. Med. 31 (10) (2001) 1254–1262.

[28] S.L. Hazen, Myeloperoxidase and plaque vulnerability, Arterioscler. Thromb. Vasc. Biol. 24 (7) (2004) 1143–1146.

[29] A. Daugherty, J.L. Dunn, D.L. Rateri, J.W. Heinecke, Myeloperoxidase, a catalyst for lipoprotein oxidation, is expressed in human atherosclerotic lesions, J. Clin. Investig. 94 (1) (1994) 437–444.

[30] S.J. Nicholls, W.H. Tang, D. Brennan, M.L. Brennan, S. Mann, S.E. Nissen, S.L. Hazen, Risk prediction with serial myeloperoxidase monitoring in patients with acute chest pain, Clin. Chem. 57 (12) (2011) 1762–1770.

[31] W.H. Tang, Y. Wu, S.J. Nicholls, S.L. Hazen, Plasma myeloperoxidase predicts incident cardiovascular risks in stable patients undergoing medical management for coronary artery disease, Clin. Chem. 57 (1) (2011) 33–39.

[32] V. Rudolph, B.U. Goldmann, C. Bos, T.K. Rudolph, A. Klinke, K. Friedrichs, D. Lau, K. Wegscheider, M. Haddad, T. Meinertz, S. Baldus, Diagnostic value of MPO plasma levels in patients admitted for suspected myocardial infarction, Int. J. Cardiol. 153 (3) (2011) 267–271.

[33] I. Rashid, G.J. Maghzal, Y.-C. Chen, D. Cheng, J. Talib, D. Newington, M. Ren, S.K. Vajandar, A. Searle, A. Maluenda, E.-L. Lindstedt, A. Jabbour, A.J. Kettle, A. Bongers, C. Power, E. Michaëlsson, K. Peter, R. Stocker, Myeloperoxidase is a potential molecular imaging and therapeutic target for the identification and stabilization of high-risk atherosclerotic plaque, Eur. Heart J. 39 (35) (2018) 3301–3310.

[34] E. Malle, G. Waeg, R. Schreiber, E.F. Gröne, W. Sattler, H.-J. Gröne, Immunohistochemical evidence for the myeloperoxidase/H2O2/halide system in human atherosclerotic lesions, Eur. J. Biochem. 267 (14) (2001) 4495–4503.

[35] T. Lazarevic-Pasti, A. Leskovac, V. Vasic, Myeloperoxidase inhibitors as potential drugs, Curr. Drug Metabol. 16 (3) (2015) 168–190.

[36] A.J. Kettle, C.A. Gedye, M.B. Hampton, C.C. Winterbourn, Inhibition of myeloperoxidase by benzoic acid hydrazides, Biochem. J. 308 (Pt 2) (1995) 559–563 Pt 2.

[37] A.K. Tiden, T. Sjogren, M. Svensson, A. Bernlind, R. Senthilmohan, F. Auchere, H. Norman, P.O. Markgren, S. Gustavsson, S. Schmidt, S. Lundquist, L.V. Forbes, N.J. Magon, L.N. Paton, G.N. Jameson, H. Eriksson, A.J. Kettle, 2-thioxanthines are mechanism-based inactivators of myeloperoxidase that block oxidative stress during inflammation, J. Biol. Chem. 286 (43) (2011) 37578–37589.

[38] M.D. Rees, S.E. Bottle, K.E. Fairfull-Smith, E. Malle, J.M. Whitelock, M.J. Davies, Inhibition of myeloperoxidase-mediated hypochlorous acid production by nitroxides, Biochem. J. 421 (1) (2009) 79–86.

[39] M. Koelsch, R. Mallak, G.G. Graham, T. Kajer, M.K. Milligan, L.Q. Nguyen, D.W. Newsham, J.S. Keh, A.J. Kettle, K.F. Scott, J.B. Ziegler, D.I. Pattison, S. Fu, C.L. Hawkins, M.D. Rees, M.J. Davies, Acetaminophen (paracetamol) inhibits myeloperoxidase-catalyzed oxidant production and biological damage at therapeutically achievable concentrations, Biochem. Pharmacol. 79 (8) (2010) 1156–1164.

[40] J. Soubhye, I. Aldib, C. Delporte, M. Prevost, F. Dufrasne, P.V. Antwerpen, Myeloperoxidase as a target for the treatment of inflammatory syndromes: mechanisms and structure activity relationships of inhibitors, Curr. Med. Chem. 23 (35) (2016) 3975–4008.

[41] C.J. van Dalen, M.W. Whitehouse, C.C. Winterbourn, A.J. Kettle, Thiocyanate and chloride as competing substrates for myeloperoxidase, Biochem. J. 327 (Pt 2) (1997) 487–492.

[42] O. Skaff, David I. Pattison, Michael J. Davies, Hypothiocyanous acid reactivity with low-molecular-mass and protein thiols: absolute rate constants and assessment of biological relevance, Biochem. J. 422 (1) (2009) 111–117.

[43] P.E. Morgan, D.I. Pattison, J. Talib, F.A. Summers, J.A. Harmer, D.S. Celermajer, C.L. Hawkins, M.J. Davies, High plasma thiocyanate levels in smokers are a key determinant of thiol oxidation induced by myeloperoxidase, Free Radic. Biol. Med. 51 (9) (2011) 1815–1822.

[44] J. Talib, D.I. Pattison, J.A. Harmer, D.S. Celermajer, M.J. Davies, High plasma thiocyanate levels modulate protein damage induced by myeloperoxidase and perturb measurement of 3-chlorotyrosine, Free Radic. Biol. Med. 53 (1) (2012) 20–29.

[45] P.E. Morgan, R.P. Laura, R.A. Maki, W.F. Reynolds, M.J. Davies, Thiocyanate supplementation decreases atherosclerotic plaque in mice expressing human myeloperoxidase, Free Radic. Res. 49 (6) (2015) 743–749.

[46] P.E. Nedoboy, P.E. Morgan, T.J. Mocatta, A.M. Richards, C.C. Winterbourn, M.J. Davies, High plasma thiocyanate levels are associated with enhanced myeloperoxidase-induced thiol oxidation and long-term survival in subjects following a first myocardial infarction, Free Radic. Res. 48 (10) (2014) 1256–1266.

[47] J. Arnold, E. Monzani, P.G. Furtmüller, M. Zederbauer, L. Casella, C. Obinger, Kinetics and thermodynamics of halide and nitrite oxidation by mammalian heme peroxidases, Eur. J. Inorg. Chem. 19 (2006) 3801–3811 2006.

[48] S.A. Hoption Cann, Hypothesis: dietary iodine intake in the etiology of cardiovascular disease, J. Am. Coll. Nutr. 25 (1) (2006) 1–11.

[49] H.V. Tran, N.A. Erskine, C.I. Kiefe, B.A. Barton, K.L. Lapane, V.T.H. Do, R.J. Goldberg, Is low iodine a risk factor for cardiovascular disease in Americans without thyroid dysfunction? Findings from NHANES, Nutr. Metab. Cardiovasc. Dis. 27 (7) (2017) 651–656.

[50] A. Iwata, M.L. Morrison, M.B. Roth, Iodide protects heart tissue from reperfusion injury, PLoS One 9 (11) (2014) e112458.

[51] R.A. Matthijsen, D. Huugen, N.T. Hoebers, B. de Vries, C.J. Peutz-Kootstra, Y. Aratani, M.R. Daha, J.W.C. Tervaert, W.A. Buurman, P. Heeringa, Myeloperoxidase is critically involved in the induction of organ damage after renal ischemia reperfusion, Am. J. Pathol. 171 (6) (2007) 1743–1752.

[52] C. Lentner, Geigy Scientific Tables: Physical Chemistry, Composition of Blood, Hematology, Somatometric Data, Ciba-Geigy Ltd, Basle, 1984.

[53] D.F. Gardner, R.M. Centor, R.D. Utiger, Effects of low dose oral iodide supplementation on thyroid function in normal men, Clin. Endocrinol. 28 (3) (1988) 283–288.

[54] J.B. Sterling, W.R. Heymann, Potassium iodide in dermatology: a 19th century drug for the 21st century-uses, pharmacology, adverse effects, and contraindications, J. Am. Acad. Dermatol. 43 (4) (2000) 691–697.

[55] E. Malle, L. Hazell, R. Stocker, W. Sattler, H. Esterbauer, G. Waeg, Immunologic detection and measurement of hypochlorite-modified LDL with specific monoclonal antibodies, Arterioscler. Thromb. Vasc. Biol. 15 (7) (1995) 982–989.

[56] C.L. Hawkins, P.E. Morgan, M.J. Davies, Quantification of protein modification by oxidants, Free Radic. Biol. Med. 46 (8) (2009) 965–988.

[57] R. Garcia-Arrona, M. Arranz, A. Bordagaray, E. Millán, Practical activity for development and validation of a simple UV-spectroscopic method for iodate determination in table salt, J. Lab. Chemical Educ. 5 (2) (2017) 26–31.

[58] T. Nybo, H. Cai, C.Y. Chuang, L.F. Gamon, A. Rogowska-Wrzesinska, M.J. Davies, Chlorination and oxidation of human plasma fibronectin by myeloperoxidase-derived oxidants, and its consequences for smooth muscle cell function, Redox Biol. 19 (2018) 388–400.

[59] S. Vanichkitrungruang, C.Y. Chuang, C.L. Hawkins, A. Hammer, G. Hoefler, E. Malle, M.J. Davies, Oxidation of human plasma fibronectin by inflammatory oxidants perturbs endothelial cell function, Free Radic. Biol. Med. 136 (2019) 118–134.

[60] E. Malle, G. Waeg, R. Schreiber, E.F. Grone, W. Sattler, H.J. Grone, Immunohistochemical evidence for the myeloperoxidase/H2O2/halide system in human atherosclerotic lesions: colocalization of myeloperoxidase and hypochlorite-modified proteins, Eur. J. Biochem. 267 (14) (2000) 4495–4503.

[61] G. Marsche, A. Hammer, O. Oskolkova, K.F. Kozarsky, W. Sattler, E. Malle, Hypochlorite-modified high density lipoprotein, a high affinity ligand to scavenger receptor class B, type I, impairs high density lipoprotein-dependent selective lipid uptake and reverse cholesterol transport, J. Biol. Chem. 277 (35) (2002) 32172–32179.

[62] A. Hammer, G. Desoye, G. Dohr, W. Sattler, E. Malle, Myeloperoxidase-dependent generation of hypochlorite-modified proteins in human placental tissues during normal pregnancy, Lab. Investig. 81 (4) (2001) 543–554.

[63] T. Nybo, S. Dieterich, L.F. Gamon, C.Y. Chuang, A. Hammer, G. Hoefler, E. Malle, A. Rogowska-Wrzesinska, M.J. Davies, Chlorination and oxidation of the extracellular matrix protein laminin and basement membrane extracts by hypochlorous acid and myeloperoxidase, Redox Biol. 20 (2019) 496–513.

[64] T.R. Thomas, D.T. Pence, R.A. Hasty, The disproportionation of hypoiodous acid, J. Inorg. Nucl. Chem. 42 (2) (1980) 183–186.

[65] J. Li, J. Jiang, Y. Zhou, S.-Y. Pang, Y. Gao, C. Jiang, J. Ma, Y. Jin, Y. Yang, G. Liu, L. Wang, C. Guan, Kinetics of oxidation of iodide (I–) and hypoiodous acid (HOI) by peroxymonosulfate (PMS) and formation of iodinated products in the PMS/I–/NOM system, Environ. Sci. Technol. Lett. 4 (2) (2017) 76–82.

[66] Y. Bichsel, U. von Gunten, Oxidation of iodide and hypoiodous acid in the disinfection of natural waters, Environ. Sci. Technol. 33 (22) (1999) 4040–4045.

[67] R.K. Schindhelm, L.P. van der Zwan, T. Teerlink, P.G. Scheffer, Myeloperoxidase: a useful biomarker for cardiovascular disease risk stratification? Clin. Chem. 55 (8) (2009) 1462–1470.

[68] J.D. Chandler, B.J. Day, Biochemical mechanisms and therapeutic potential of pseudohalide thiocyanate in human health, Free Radic. Res. 49 (6) (2015) 695–710.

[69] J.D. Chandler, E. Min, J. Huang, C.S. McElroy, N. Dickerhof, T. Mocatta, A.A. Fletcher, C.M. Evans, L. Liang, M. Patel, A.J. Kettle, D.P. Nichols, B.J. Day, Antiinflammatory and antimicrobial effects of thiocyanate in a cystic fibrosis mouse model, Am. J. Respir. Cell Mol. Biol. 53 (2) (2015) 193–205.

[70] B. Di Jeso, P. Arvan, Thyroglobulin from molecular and cellular biology to clinical endocrinology, Endocr. Rev. 37 (1) (2016) 2–36.

[71] P.J. O'Brien, Peroxidases, Chem. Biol. Interact. 129 (1–2) (2000) 113–139.

[72] N. Carrasco, Iodide transport in the thyroid gland, Biochim. Biophys. Acta 1154 (1) (1993) 65–82.

[73] B.A. Rousset, How iodide reaches its site of utilisation in the thyroid gland; involvement of solute carrier 26A4 (pendrin) and solute carrier 5A8 (apical iodide transporter), Eur. Endocrinol. 1 (2007) 81–82.

[74] Michael J. Davies, Protein oxidation and peroxidation, Biochem. J. 473 (Pt 7) (2016) 805–825.

[75] E.L. Thomas, M.B. Grisham, M.M. Jefferson, Preparation and characterization of chloramines, Methods Enzymol. 132 (1986) 569–585.

[76] F. Afshinnia, L. Zeng, J. Byun, C.A. Gadegbeku, M.C. Magnone, C. Whatling, B. Valastro, M. Kretzler, S. Pennathur, Myeloperoxidase levels and its product 3-chlorotyrosine predict chronic kidney disease severity and associated coronary

artery disease, Am. J. Nephrol. 46 (1) (2017) 73–81.

[77] S. Baldus, J.P. Eiserich, M.-L. Brennan, R.M. Jackson, C.B. Alexander, B.A. Freeman, Spatial mapping of pulmonary and vascular nitrotyrosine reveals the pivotal role of myeloperoxidase as a catalyst for tyrosine nitration in inflammatory diseases, Free Radic. Biol. Med. 33 (7) (2002) 1010–1019.

[78] M.L. Morrison, A. Iwata, C.C. Keyes, W. Langston, M.A. Insko, L.A. Langdale, M.B. Roth, Iodide improves outcome after acute myocardial infarction in rats and pigs, Crit. Care Med. 46 (11) (2018).

[79] C. Storkey, M.J. Davies, D.I. Pattison, Reevaluation of the rate constants for the reaction of hypochlorous acid (HOCl) with cysteine, methionine, and peptide derivatives using a new competition kinetic approach, Free Radic. Biol. Med. 73 (2014) 60–66.

[80] G.T.F. Wong, L.-S. Zhang, The kinetics of the reactions between iodide and hydrogen peroxide in seawater, Mar. Chem. 111 (1) (2008) 22–29.

[81] A. Armstrong David, E. Huie Robert, H. Koppenol Willem, V. Lymar Sergei, G. Merényi, P. Neta, B. Ruscic, M. Stanbury David, S. Steenken, P. Wardman, Standard electrode potentials involving radicals in aqueous solution: inorganic radicals (IUPAC Technical Report), Pure Appl. Chem. (2015) 1139.